

# Dalton Transactions

An international journal of inorganic chemistry

Accepted Manuscript

This article can be cited before page numbers have been issued, to do this please use: G. Bergamini and M. Natali, *Dalton Trans.*, 2019, DOI: 10.1039/C9DT02846C.



This is an Accepted Manuscript, which has been through the Royal Society of Chemistry peer review process and has been accepted for publication.

Accepted Manuscripts are published online shortly after acceptance, before technical editing, formatting and proof reading. Using this free service, authors can make their results available to the community, in citable form, before we publish the edited article. We will replace this Accepted Manuscript with the edited and formatted Advance Article as soon as it is available.

You can find more information about Accepted Manuscripts in the [Information for Authors](#).

Please note that technical editing may introduce minor changes to the text and/or graphics, which may alter content. The journal's standard [Terms & Conditions](#) and the [Ethical guidelines](#) still apply. In no event shall the Royal Society of Chemistry be held responsible for any errors or omissions in this Accepted Manuscript or any consequences arising from the use of any information it contains.

## ARTICLE

# Homogeneous vs. heterogeneous catalysis for hydrogen evolution by a nickel(II) bis(diphosphine) complex

Giovanni Bergamini <sup>a</sup> and Mirco Natali <sup>\*a</sup>Received 00th January 20xx,  
Accepted 00th January 20xx

DOI: 10.1039/x0xx00000x

The nickel(II) bis(diphosphine) complex **1** bearing carboxylic acid functional groups at the periphery has been prepared and characterized. Its catalytic ability towards the hydrogen evolution reaction (HER) has been evaluated under different experimental conditions: i) under homogeneous electrocatalysis in acetonitrile using trifluoroacetic acid as the proton source, ii) under homogeneous photocatalysis in aqueous solution using Ru(bpy)<sub>3</sub><sup>2+</sup> (where bpy = 2,2'-bipyridine) as the sensitizer and ascorbic acid as the sacrificial electron donor, and iii) under heterogeneous electrochemical conditions upon grafting onto mesoporous TiO<sub>2</sub>. The results show that complex **1** is a competent and efficient catalyst for the HER under homogeneous conditions, both electro- and photochemical ones, while undergoes rapid deactivation once attached onto the TiO<sub>2</sub> surface. This is attributed to both catalyst binding mode and structural rigidity imparted by the covalent grafting which highlights how catalyst design has to be considered for direct transposition of molecular catalysis onto (photo)electrode surfaces.

## Introduction

The increasing of the energy demand due to population growth and technological development requires a scientific challenge based on the implementation of renewable energy sources. Direct storage of energy into chemical bonds with the production of "chemical fuels" represents a flexible approach to overcome the intrinsic inhomogeneity of natural sources such as solar energy.<sup>1,2</sup> The simplest chemical reaction that allows for a direct interconversion between external energy and chemical energy is represented by the formation of a hydrogen molecule via proton reduction (eq 1).



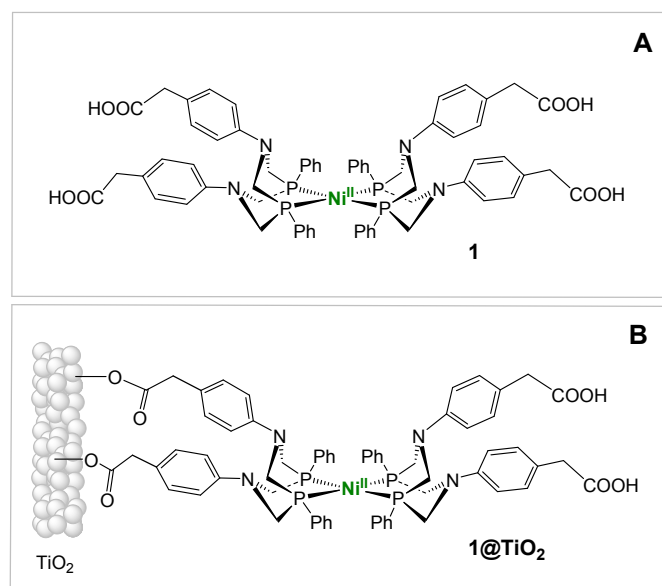
In nature, microalgae and bacteria are capable of performing such a reversible chemical transformation by means of natural enzymes called hydrogenases featuring active sites based on iron and/or nickel clusters.<sup>3,4</sup> Many artificial molecular analogues have been synthesized and characterized which can mimic the natural functions and produce hydrogen via proton reduction under both electrochemical and light-driven conditions.<sup>5,6</sup> Some examples include hydrogenase mimics,<sup>7,8</sup> cobaloximes and cobalt diimine complexes,<sup>9-11</sup> cobalt and iron porphyrins,<sup>12-16</sup> polypyridine complexes based on iron, cobalt, and nickel.<sup>17-23</sup>

Nickel(II) bis(diphosphine) complexes, known as 'DuBois' catalysts, have received considerable attention in the last years. These compounds, with the general formula [Ni<sup>II</sup>(P<sub>2</sub><sup>R</sup>N<sub>2</sub><sup>R'</sup>)<sub>2</sub>](BF<sub>4</sub>)<sub>2</sub> (where R, R' are aliphatic and/or aromatic groups), display pendant amines that functions as proton relays and assist the protonation steps during the hydrogen evolution mechanism,<sup>24</sup> providing small overpotentials for catalysing proton reduction. Their characteristic and favourable properties towards hydrogen evolution catalysis have stimulated many interests on both a fundamental and applicative standpoint. Many molecular analogues, based on different R and R' functionalities and/or diverse ligand architectures,<sup>25-29</sup> have been indeed prepared and studied in terms of their electrocatalytic properties showing TOFs above 100,000 s<sup>-1</sup>.<sup>29</sup> At the same time, other nickel(II) bis(diphosphine) complexes have been synthesized and used in combination with diverse materials for the construction of both electro- and photo-active systems.<sup>30-37</sup> In spite of the apparent versatility of the class of the nickel(II) 'DuBois' catalysts, direct comparisons of the catalytic properties of the same compound under different experimental conditions are rare.<sup>35</sup> In this work we have prepared the complex [Ni<sup>II</sup>(P<sub>2</sub><sup>Ph</sup>N<sub>2</sub><sup>PhCH<sub>2</sub>COOH</sup>)<sub>2</sub>](BF<sub>4</sub>)<sub>2</sub> (**1**, Scheme 1A) and studied its behaviour as a hydrogen evolving catalyst (HEC) under three different conditions: i) under homogenous electrocatalysis in acetonitrile as the solvent using trifluoroacetic acid (TFA) as the proton source, ii) under homogenous photocatalysis in aqueous solution using Ru(bpy)<sub>3</sub><sup>2+</sup> (where bpy = 2,2'-bipyridine) as the sensitizer and ascorbic acid as the sacrificial electron donor, and iii) under heterogeneous electrocatalysis in aqueous solution by grafting the nickel complex onto the surface of mesoporous TiO<sub>2</sub> (**1@TiO<sub>2</sub>**, Scheme 1B). The results show that the present compound displays good catalytic properties under homogenous conditions (conditions i and ii), while shows a

<sup>a</sup> Department of Chemical and Pharmaceutical Sciences, University of Ferrara, Via L. Borsari 46, 44121, Ferrara, Italy. E-mail: [mirco.natali@unife.it](mailto:mirco.natali@unife.it)

Electronic Supplementary Information (ESI) available: characterization of the ligand and complex **1**, details of the electrocatalytic characterization, details of the photocatalytic experiments, details of the characterization of **1** onto TiO<sub>2</sub>. See DOI: 10.1039/x0xx00000x

rapid deactivation leading to inefficient catalysis under heterogeneous ones (condition iii). The data reported herein thus point out how a suitable catalyst design is important in order to apply a certain system under specific experimental conditions.



**Scheme 1.** (A) Molecular structure of complex **1**; (B) schematic representation of the functionalization of mesoporous  $\text{TiO}_2$  thin films with **1**.

## Experimental section

### Materials and methods.

All reagents were of reagent grade quality and purchased from commercial suppliers (Sigma Aldrich, Alfa Aesar). Anhydrous acetonitrile was used for the electrochemical characterization. MilliQ ultrapure water was used for electrochemical and photochemical studies in aqueous solutions. FTO-covered glass slides (20 cm  $\times$  20 cm, TEC 8, 8  $\Omega$ /cm) were purchased from Pilkington. A commercial  $\text{TiO}_2$  paste (18NR-T, GreatCell-Solar) was used for the preparation of the  $\text{TiO}_2$  thin films.

### Apparatus and procedures.

NMR spectra were collected on a Bruker Avance 300 MHz spectrometer. Diffuse reflectance IR spectra were obtained using a Bruker Vertex 10 FT-IR spectrometer. UV-Vis absorption spectra were recorded on a Jasco V-570 UV/Vis/NIR spectrophotometer. Emission spectra were taken on an Edinburgh Instrument spectrofluorometer equipped with a 900 W xenon arc lamp as excitation source, a photomultiplier tube, and an InGaAs detector for the visible and the NIR detection, respectively. Nanosecond transient absorption measurements were performed with a custom laser spectrometer comprised of a Continuum Surelite II Nd:YAG laser (FWHM = 8 ns) with frequency doubled (532 nm, 330 mJ) option, an Applied Photophysics xenon light source including a mod. 720 150 W lamp housing, a mod. 620 power-controlled lamp supply and a mod. 03 - 102 arc lamp pulser. Laser excitation was provided at 90° with respect to the white light probe beam. Light transmitted by the

sample was focused onto the entrance slit of a 300 mm focal length Acton SpectraPro 2300i triple grating, flat field, double exit monochromator equipped with a photomultiplier detector (Hamamatsu R3896). Signals from the photomultiplier (kinetic traces) were processed by means of a TeledyneLeCroy 604Zi (400 MHz, 20 GS/s) digital oscilloscope. Before all the measurements the solutions were purged with nitrogen for 10 minutes. Electrochemical measurements were carried out with a PC-interfaced Eco Chemie Autolab/Pgstat 30 Potentiostat. In cyclic voltammetry experiments, a conventional three-electrode cell assembly was adopted: a glassy carbon (GC, 7 mm<sup>2</sup> surface area) and a platinum electrode were used as the working and counter electrodes, respectively. A bare silver wire was used as a quasi-reference, potentials were then referenced to ferrocene, added as an internal standard. All experiments were performed in nitrogen-purged acetonitrile solutions using  $\text{TBAPF}_6$  as the supporting electrolyte.  $\text{TBAPF}_6$  powder was dried overnight in an oven at 60°C before preparation of the electrolyte solution. The GC electrode was accurately polished with alumina slurry before every scan. Potential controlled electrolysis experiments were performed in a gas-tight custom-made electrochemical cell using a large surface area carbon rod as the working electrode, a platinum grid as the counter electrode (separated from the test solution by a frit) and a saturated calomel electrode (SCE, Amel) as the reference electrode. The headspace of the cell was connected to the gas chromatography apparatus described below for the determination and quantification of hydrogen. Electrochemical experiments in aqueous solutions were performed in the same cell by replacing the GC working electrode with the functionalized glass slide and using a SCE as the reference electrode. The photochemical hydrogen evolution experiments were carried out upon continuous visible-light irradiation of a reactor containing the solution (a 10 mm pathlength pyrex glass cuvette with head space obtained from a round-bottom flask). A solar simulator (Abet Technologies) was used as the light source and a cut-off filter at  $\lambda < 400$  nm was employed. The gas phase of the reaction vessel was analysed on an Agilent Technologies 490 microGC equipped with a 5 Å molecular sieve column (10 m), a thermal conductivity detector, and using argon as carrier gas. Additional details of the setup and procedures used for the hydrogen evolution experiments can be found in previous reports.<sup>11</sup>

### Synthetic procedures.

The syntheses of the nickel complexes were performed under nitrogen using the Schlenk technique according to literature procedures.<sup>26,33,38</sup>

**Synthesis of ligand  $\text{P}_2^{\text{Ph}}\text{N}_2^{\text{PhCH}_2\text{COOH}}$ .**<sup>33a</sup> In 25 mL degassed ethanol 180 mg (6.0 mmol) *para*formaldehyde and phenylphosphine (10% in hexane, 3.3 mL, 3.0 mmol) were added. The mixture was stirred at 80°C until the solution became transparent. Then, 453 mg (3.0 mmol) 4-(aminophenyl)acetic acid were added and the solution was refluxed overnight under continuous stirring. Subsequently, the solution was cooled down to room temperature. The white precipitate was collected on a frit and washed with cold ethanol. Yield: 50%. <sup>1</sup>H-NMR (300 MHz, DMSO-*d*<sup>6</sup>): 3.30 (s, 4H, Ph-CH<sub>2</sub>-COOH), 4.07-4.11 (t, 4H, P-CH<sub>2</sub>-N), 4.48-4.52 (dd, 4H, P-

CH<sub>2</sub>-N), 6.57-6.59 (d, 4H, NC<sub>6</sub>H<sub>4</sub>), 7.02 (d, 4H, NC<sub>6</sub>H<sub>4</sub>), 7.45-7.49 (m, 6H, PC<sub>6</sub>H<sub>5</sub>), 7.51-7.67 (m, 4H, PC<sub>6</sub>H<sub>5</sub>), 12.05 ppm (s, 2H, COOH); <sup>31</sup>P-NMR (300 MHz, DMSO-d<sub>6</sub>): -50.15 ppm. FT-IR (KBr pellet): 3000 cm<sup>-1</sup>, 1730 cm<sup>-1</sup>.

**Synthesis of the Ni(ACN)<sub>6</sub>(BF<sub>4</sub>)<sub>2</sub> precursor.**<sup>38</sup> In 30 mL acetonitrile 0.5 g (0.85 mmol) Ni powder and 2.0 g (17 mmol) NOBF<sub>4</sub> were added. The mixture was left under stirring for 2 hours until the solution became deep blue coloured. The mixture was filtered and diethyl ether was added to the solution to favour precipitation. The nickel salt was collected on a frit and washed with diethyl ether.

**Synthesis of complex Ni<sup>II</sup>(P<sub>2</sub><sup>Ph</sup>N<sub>2</sub><sup>PhCH<sub>2</sub>COOH</sup>)(BF<sub>4</sub>)<sub>2</sub> (**1**).**<sup>26</sup> In 5 mL acetonitrile 128 mg (0.2 mmol) ligand P<sub>2</sub><sup>Ph</sup>N<sub>2</sub><sup>PhCH<sub>2</sub>COOH</sup> and 50 mg (0.1 mmol) Ni(ACN)<sub>6</sub>(BF<sub>4</sub>)<sub>2</sub> precursor were added. The solution was left under continuous stirring for 3 hours. The red solution was then concentrated under vacuum and diethyl ether was added to allow precipitation of the desired complex. The solid was collected on a frit and washed with diethyl ether. Yield: 85%. <sup>1</sup>H-NMR (300 MHz, ACN-d<sub>3</sub>): 3.65 (s, 8H, Ph-CH<sub>2</sub>-COOH), 3.98 (d, 8H, PCH<sub>2</sub>N), 4.20 (d, 8H, PCH<sub>2</sub>N), 7.18 (d, 12H, NC<sub>6</sub>H<sub>4</sub>), 7.38 (d, 12H, NC<sub>6</sub>H<sub>4</sub>), 7.46 (m, 4H, PC<sub>6</sub>H<sub>5</sub>), 9.20 ppm (s, br, 4H, COOH); <sup>31</sup>P-NMR (300 MHz, ACN-d<sub>3</sub>): 3.47 ppm. UV-Vis: 479 nm. FT-IR (KBr pellet): 3000 cm<sup>-1</sup>, 1730 cm<sup>-1</sup>.

#### Preparation of TiO<sub>2</sub> electrodes.

Mesoporous TiO<sub>2</sub> thin films (1 cm<sup>2</sup> surface area) were prepared by doctor-blading of the TiO<sub>2</sub> paste onto FTO glass slides using a Scotch tape mask, followed by calcination at 450°C for 30 minutes. Prior to deposition of the TiO<sub>2</sub> paste the FTO film was polished using Alconox detergent and isopropyl alcohol. Direct functionalization with complex **1** (**1@TiO<sub>2</sub>**, Scheme 1B) was achieved at room temperature by leaving the TiO<sub>2</sub> electrodes overnight into a 1 mM solution of **1** in acetonitrile. The functionalized electrodes **1@TiO<sub>2</sub>** were then washed with acetonitrile and dried under a stream of air. The functionalization was confirmed by diffuse reflectance IR spectroscopy of samples obtained by mixing scraped **1@TiO<sub>2</sub>** films with KBr. The coverage was quantified using a reported procedure involving immersion of the electrodes into a 0.1 M NaOH solution followed by spectrophotometric analysis of the resultant solution.<sup>31a</sup> The value obtained is an average of three different electrode tested.

## Results and discussion

### Synthesis and characterization.

Compounds **1** has been prepared by adopting literature protocols<sup>26,33,38</sup> and characterized by <sup>1</sup>H-NMR, <sup>31</sup>P-NMR, UV-Vis spectroscopy, and IR spectroscopy (Figure S1-S5). The results are fully consistent with those obtained in previous reports.<sup>33</sup> Cyclic voltammetry (CV) experiments have been performed to characterize the electrochemical properties of complex **1** in acetonitrile. Upon cathodic scan, complex **1** displays two irreversible cathodic processes with peak potentials at -0.89 V and -1.05 V vs. Fc/Fc<sup>+</sup> (Figure S6) which can be attributed to consecutive reductions at the metal centre, namely Ni(II)/Ni(I)

and Ni(I)/Ni(0), respectively, by analogy with the processes observed in similar nickel(II) bis(diphosphine) complexes.<sup>27</sup> The irreversible nature of the reduction processes is, however, peculiar of compound **1** and can be attributed either to the coupling of some chemical step likely promoted by the presence of the acid functionalities or to some adsorption phenomena resulting in electrode passivation. The failure to observe any anodic process during the return scan, however, prompts us to favour the latter hypothesis over the first one.

### Homogeneous electrocatalysis in acetonitrile.

Addition of trifluoroacetic acid (pK<sub>a</sub> = 12.7 in acetonitrile)<sup>39</sup> in the acetonitrile solution containing complex **1** is followed by the appearance of a catalytic wave at potentials close to the Ni(I)/Ni(0) process, whose current value (*i*<sub>cat</sub>) is dependent on the concentration of added acid (Figure 1A).

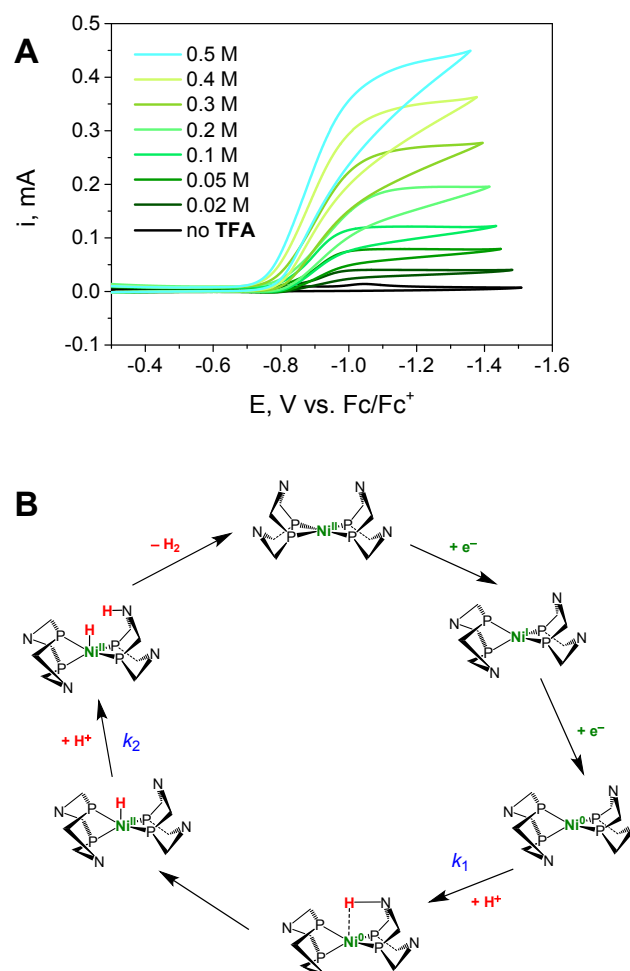


**Figure 1.** (A) CV of 1 mM **1** in acetonitrile (0.1 M TBAPF<sub>6</sub> as supporting electrolyte) at a scan rate of  $\nu = 100$  mV/s in the presence of 0-0.5 M TFA; (B) EEC catalytic mechanism for hydrogen evolution catalysed by **1** in acetonitrile with TFA as the proton source.

This electrochemical response can be ascribed to electrocatalytic proton reduction promoted by the nickel(II) complex. This attribution is further confirmed by bulk electrolysis experiments conducted at -1.20 V vs. Fc/Fc<sup>+</sup> which

show the progressive formation of hydrogen without appreciable degradation of the sample during a 2-hour experiment. A Faradaic efficiency (FE) of 77% has been obtained under these conditions (Figure S7). An overpotential of  $\eta = 0.32(\pm 0.03)$  can be estimated from the comparison of the mid-wave potential ( $-0.93$  V vs.  $\text{Fc}/\text{Fc}^+$ ) and the thermodynamic potential for the reduction of TFA in acetonitrile ( $-0.61$  V vs.  $\text{Fc}/\text{Fc}^+$ ) estimated using literature protocols.<sup>40</sup> Interestingly, the mid-wave potential is appreciably constant upon increasing the concentration of TFA up to 0.5 M and positive than the  $\text{Ni}(\text{I})/\text{Ni}(\text{O})$  half-wave potential of  $E_{1/2} = -1.00$  V vs.  $\text{Fc}/\text{Fc}^+$  (as possibly extracted from the second cathodic wave of **1** in the absence of TFA, when the current is half the peak value). These results are compatible with hydrogen evolution catalysis occurring via an EECC mechanism (Figure 1B) in which the second protonation step ( $k_2$ ) is rate-limiting.<sup>41</sup> This result is in line with those reported earlier by DuBois and co-workers on similar nickel bis(diphosphine) complexes using protonated DMF ( $\text{pK}_a = 6.1$  in acetonitrile)<sup>39</sup> as the acid.<sup>26-28</sup> In those cases, however, an ECEC pathway was also found to be competitive with the EECC mechanism most likely as the result of the stronger acidity of the proton source used ( $\text{DMFH}^+$  vs. TFA). Foot-of-the-wave analysis (FOWA)<sup>42</sup> has been then used to extract kinetic information from the cyclic voltammetry data. A rate-constant for the first protonation step of  $k_1 = 1.4(\pm 0.2) \times 10^5 \text{ M}^{-1}\text{s}^{-1}$  can be estimated from the linear fitting of the CV response near the foot of the wave, while a rate-constant for the second protonation step of  $k_2 = 7.8(\pm 0.8) \times 10^2 \text{ M}^{-1}\text{s}^{-1}$  can be obtained from the difference between the mid-wave potential and the half-wave potential of the  $\text{Ni}(\text{I})/\text{Ni}(\text{O})$  redox couple in **1** (see ESI for details).<sup>41</sup> Interestingly, the value obtained is comparable with the one measured by a stopped-flow technique for the protonation of a related nickel(II)-hydride species with acids of moderate strength.<sup>43</sup>

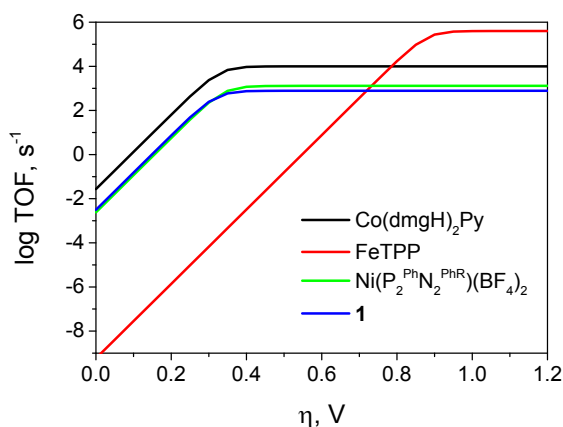


**Figure 2.** Tafel plot analysis of the electrocatalytic property of complex **1** in acetonitrile using TFA (1 M) as the proton source (blue) and comparison with reference literature systems: (black) cobaloxime in DMF,  $\text{Et}_3\text{NH}^+$  (1 M) as the acid;<sup>45</sup> (red) iron tetraphenylporphyrin in DMF,  $\text{Et}_3\text{NH}^+$  (1 M) as the acid;<sup>15</sup> (green)  $\text{Ni}^{\text{II}}(\text{P}_2^{\text{Ph}}\text{N}_2^{\text{PhR}})(\text{BF}_4)_2$  in acetonitrile ( $\text{R} = -\text{CH}_2\text{P}(\text{O})(\text{OEt})_2$ ),  $\text{DMFH}^+$  (1 M) as the acid.<sup>26</sup>

Tafel plot analysis<sup>44</sup> has been then used to benchmark the present system with a parent nickel complex and other

molecular electrocatalysts reported in the literature (Figure 2). Although high catalysis rates (TOFs) cannot be achieved when compared to other catalysts such as cobaloximes and iron porphyrins, complex **1** displays an appreciably low overpotential. Interestingly, its electrocatalytic behaviour is comparable to that recorded for a nickel(II) bis(diphosphine) analogue bearing phosphonic ester groups (green traces in Figure 2).

### Homogeneous photocatalysis in aqueous solution.

The ability of complex **1** to promote catalytic hydrogen evolution has been then assessed under homogeneous photochemical conditions by using a three-component system involving  $\text{Ru}(\text{bpy})_3^{2+}$  as the photosensitizer, ascorbic acid as the sacrificial donor, and **1** as the catalyst. We first checked the effect of the pH on hydrogen evolution by irradiating 5 mL of aqueous solutions containing 50  $\mu\text{M}$  **1**, 0.5 mM  $\text{Ru}(\text{bpy})_3^{2+}$ , and 0.5 M ascorbic acid and changing the pH between 3 and 6 upon addition of small aliquots of a concentrated NaOH solution. Consistently with the results obtained previously for a water-soluble nickel analogue,<sup>46</sup> the optimum pH has been found at 5 (Figure S9).

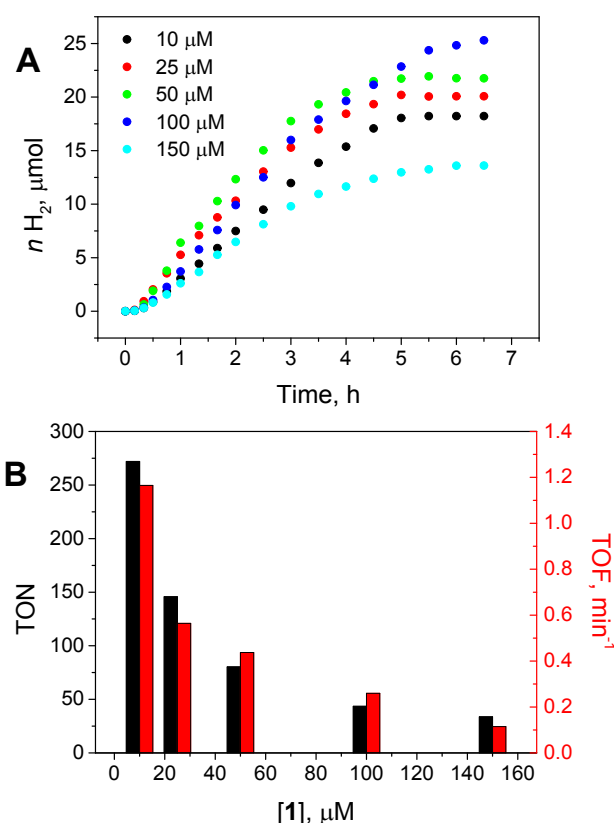


**Figure 3.** (A) Kinetics of photoinduced hydrogen evolution from 5 mL aqueous solutions containing 10-150  $\mu\text{M}$  **1**, 0.5 mM  $\text{Ru}(\text{bpy})_3\text{Cl}_2 \cdot 6\text{H}_2\text{O}$ , and 0.5 M ascorbic acid at pH 5; (B) relevant photocatalytic data at pH 5 as a function of catalyst concentration.

We then explored the photocatalytic activity towards hydrogen evolution at pH 5 by changing the catalyst concentration within the range 10-150  $\mu\text{M}$ . The kinetic traces are reported in Figure

3A, while relevant photocatalytic data are collected in Figure 3B. Hydrogen formation levels off after 6-7 hour of continuous irradiation with visible light with the best results in terms of both amount of hydrogen evolved and production rate attained at 100  $\mu\text{M}$  concentration of **1** (see ESI for additional details). Interestingly, remarkable maximum TONs up to 272 with maximum TOFs up to  $1.14 \text{ min}^{-1}$  can be estimated for the present photochemical system at the lowest concentration of **1**. Overall, the performances are comparable with those of known molecular catalysts such as cobaloximes and cobalt polypyridine complexes measured under the same experimental conditions.<sup>11,21,47,48</sup> This observation thus confirms that the present nickel bis(diphosphine) complex **1** is effective in promoting efficient hydrogen evolution under homogeneous photochemical conditions, in which main limitations to the achievement of high turnover numbers are determined by degradation of the ruthenium sensitizer.<sup>18</sup>

The origin of this remarkable photochemical performance has been also investigated by means of steady-state and time-resolved optical spectroscopy. The luminescence of the  $\text{Ru}(\text{bpy})_3^{2+}$  sensitizer in water is progressively quenched upon addition of increasing amounts of **1** (Figure S10) with yields between 15-60% within the concentration range 25-150  $\mu\text{M}$ .<sup>‡</sup> On the other hand, the emission of  $\text{Ru}(\text{bpy})_3^{2+}$  is more efficiently quenched in the presence of 0.5 M ascorbic acid at pH 5 (quenching yield of ~90%, Figure S11).<sup>§</sup> These results thus suggest that the primary photoinduced process within the **1**/ $\text{Ru}(\text{bpy})_3^{2+}$ /ascorbate three-component system is the reductive quenching of the excited sensitizer by the sacrificial donor. Although reductive quenching is the dominating photochemical pathway, opposing effects from the competing quenching by complex **1** are indeed apparent in the hydrogen evolution experiments (Figure 3A). As a matter of fact, the hydrogen evolution rates show an appreciable first-order dependence at low catalyst concentration (i.e.,  $[\mathbf{1}] < 100 \mu\text{M}$ ), then reach a maximum value at  $[\mathbf{1}] = 100 \mu\text{M}$ , and finally decrease at larger concentrations (Figure S12). Not only, a progressive increase in the lag-phase to attain steady-state (i.e., linear) hydrogen evolution is observed with increasing catalyst concentration from 50  $\mu\text{M}$  to 150  $\mu\text{M}$  **1** (Figure 3A). Both these results are consistent with an improved efficiency from the competing excited state quenching by **1** with increasing concentration of the nickel complex, as expected on the basis of luminescence experiments (Figure S10), and suggest that this process, regardless of its nature (energy or electron transfer), is detrimental towards light-driven hydrogen evolution.

Transient absorption experiments have been performed to monitor the subsequent electron transfer from the reduced sensitizer to the nickel complex **1** (Figure 4).<sup>11,18,21</sup> The transient signal at 510 nm, characteristic of the reduced  $\text{Ru}(\text{bpy})_3^+$  species,<sup>48</sup> decays with kinetics which are dependent on the concentration of the nickel complex (Figure 4A), thus pointing to the occurrence of a bimolecular electron transfer process involving reduction of **1** by  $\text{Ru}(\text{bpy})_3^+$ . This attribution is further confirmed by the residual negative absorption at 510 nm left after the decay of the  $\text{Ru}(\text{bpy})_3^+$  transient (Figure 4A) which is

consistent with the bleaching of the ground-state absorption of **1**.<sup>46</sup>

DOI: 10.1039/C9DT02846C

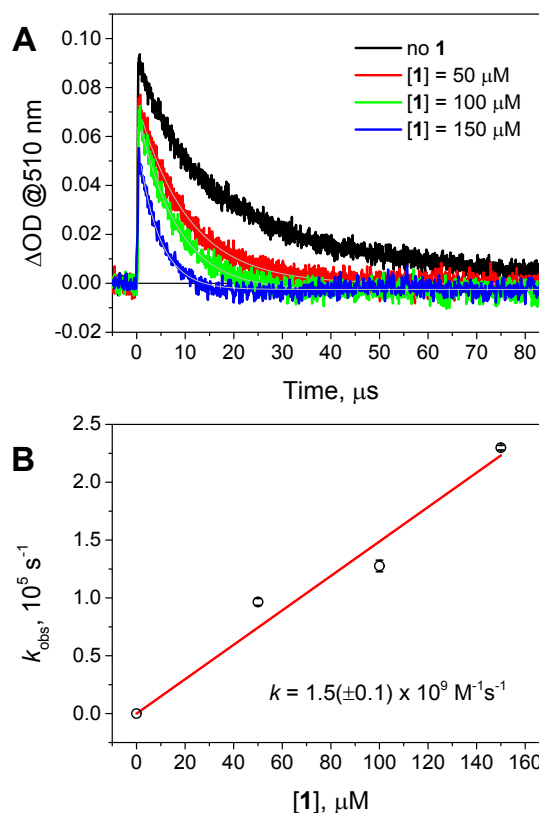


**Figure 4.** (A) Kinetic traces at 510 nm (with related single-exponential fitting) measured by laser flash photolysis (excitation at 355 nm) on aqueous solutions containing 0-150  $\mu\text{M}$  **1**, 0.07 mM  $\text{Ru}(\text{bpy})_3\text{Cl}_2 \cdot 6\text{H}_2\text{O}$ , and 0.5 M ascorbic acid at pH 5; (B) plot of the observed rate ( $k_{\text{obs}}$ ) vs.  $[\mathbf{1}]$  for the estimation of the bimolecular rate constant.

Under pseudo-first order conditions ( $[\mathbf{1}] \gg [\text{Ru}(\text{bpy})_3^+]$ ), the bimolecular rate constant for the electron transfer process from the reduced chromophore to catalyst **1** can be estimated yielding a value of  $k = 1.5(\pm 0.1) \times 10^9 \text{ M}^{-1} \text{ s}^{-1}$  (Figure 4B). This value is closed to the diffusion-controlled regime and strongly support the hypothesis that catalyst **1** is fast in promoting consecutive electron transfer processes from the photogenerated  $\text{Ru}(\text{bpy})_3^+$ . This is indeed expected based on the efficient photocatalytic activity experimentally observed, particularly at low catalyst concentrations. The decrease in the light-driven hydrogen evolution with increasing concentration of **1** above 100  $\mu\text{M}$  can be rationalized considering that, although the rate of the electron transfer process from the photogenerated  $\text{Ru}(\text{bpy})_3^+$  to **1** increases, as expected for a bimolecular process, the concomitant increase in the competitive excited state quenching of  $^*\text{Ru}(\text{bpy})_3^{2+}$  by **1** (see above) may potentially introduce additional, unfavourable channels leading to a decrease of the overall hydrogen yield. Accordingly, the best results attained at 100  $\mu\text{M}$  **1** very likely arise from a balance between favourable and detrimental effects on photocatalysis induced by the concentration of the nickel complex.

### Heterogeneous catalysis of functionalized TiO<sub>2</sub> electrodes.

The nickel(II) bis(diphosphine) complex **1** has been grafted onto mesoporous TiO<sub>2</sub> by adsorption from a 1 mM solution of **1** in acetonitrile to achieve **1@TiO<sub>2</sub>** (Scheme 1B). After overnight soaking and subsequent rinsing with acetonitrile the TiO<sub>2</sub> electrodes display a pale red colour, indicative of grafting of complex **1**. However, direct identification and quantification by UV-Vis spectroscopy is prevented by the small absorptivity of the functionalized TiO<sub>2</sub> film (molar extinction coefficient of  $\epsilon \sim 1500 \text{ M}^{-1}\text{cm}^{-1}$  at 480 nm for compound **1**)<sup>31a,33</sup> and the concomitant rise of the TiO<sub>2</sub> band-gap absorption at shorter wavelength. This notwithstanding, anchoring of complex **1** onto TiO<sub>2</sub> has been confirmed by the IR spectrum of **1@TiO<sub>2</sub>** which displays the characteristic signal of **1** at around 3000 cm<sup>-1</sup>, absent in the bare TiO<sub>2</sub> (Figure S13). Also, the IR spectra of **1@TiO<sub>2</sub>** (Figure 5) shows the shift of the C=O stretching mode towards lower frequencies (1650 cm<sup>-1</sup>) with respect to the same mode in **1** (1730 cm<sup>-1</sup>), consistent with the direct binding of the carboxylic function to the TiO<sub>2</sub> surface.<sup>49</sup> The presence of some residual signal at higher wavenumbers (shoulder with relative maximum at 1720 cm<sup>-1</sup>), compatible with that of pristine complex **1**, clearly points out that covalent grafting of **1** onto the TiO<sub>2</sub> surface does not involve all the carboxylic acid groups amongst the four available.

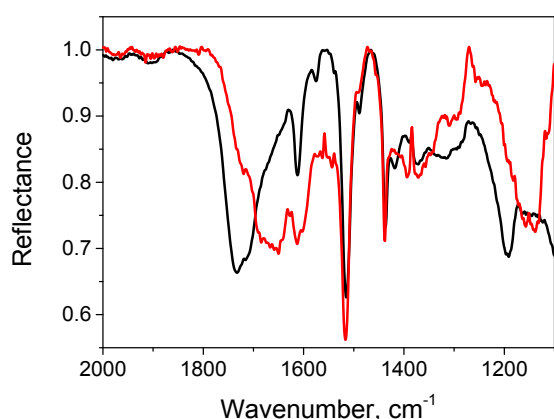


Figure 5. Comparison of the diffuse reflectance spectra (KBr pellet) of **1** (powder, black trace) and **1@TiO<sub>2</sub>** (red trace).

In order to quantify the amount of nickel complex present on the surface of the mesoporous TiO<sub>2</sub> film, we have then exploited a procedure recently reported by Reisner and co-workers.<sup>31a</sup> The electrodes have been immersed into an aqueous 0.1 M NaOH solution to irreversibly detach the nickel catalysts from the TiO<sub>2</sub> surface. This process provides a way for the direct quantification of the catalyst loading by monitoring the featuring absorption at 257 nm of the dissolved complex in solution.<sup>31a</sup> This analysis (Figure S14) yields a degree of coverage of 32.5(±0.2) nmol/cm<sup>2</sup> for **1@TiO<sub>2</sub>**. Interestingly, this value is comparable yet larger than the coverage of mesoporous TiO<sub>2</sub> by a related nickel(II) bis(diphosphine) complex bearing phosphonic acids as anchoring groups (14.6(±0.2) nmol/cm<sup>2</sup>).<sup>31a</sup> Also, the observed coverage is much larger than those of both

carbon nanotube-based electrodes (1.5 nmol/cm<sup>2</sup>)<sup>33a</sup> and glassy carbon electrodes (0.55 nmol/cm<sup>2</sup>)<sup>35</sup> prepared via covalent functionalization with a nickel bis(diphosphine) complex. In order to characterize the electrocatalytic performance of **1@TiO<sub>2</sub>**, linear sweep voltammetry has been performed at three different pH values 2, 3, and 4 on **1@TiO<sub>2</sub>** electrodes and, for comparison, on blank electrodes (bare TiO<sub>2</sub>). The data obtained at pH 3 are reported in Figure 6A, while those at pH 2 and 4 are reported in Figure S15. Overall, under cathodic scan the functionalized electrodes display larger current densities than the bare TiO<sub>2</sub> which can be attributed to the presence of the nickel complex on the surface that favours the electron transfer processes at the semiconductor/electrolyte interface resulting in hydrogen formation. An overpotential for the hydrogen evolution reaction (HER) of  $\eta = 0.36(\pm 0.05) \text{ V}$  can be estimated for **1@TiO<sub>2</sub>** at a current density value of  $J = 1 \text{ mA}$ . This value is appreciably comparable with the one measured in homogeneous electrocatalysis by **1** in acetonitrile solution using TFA as the proton source.

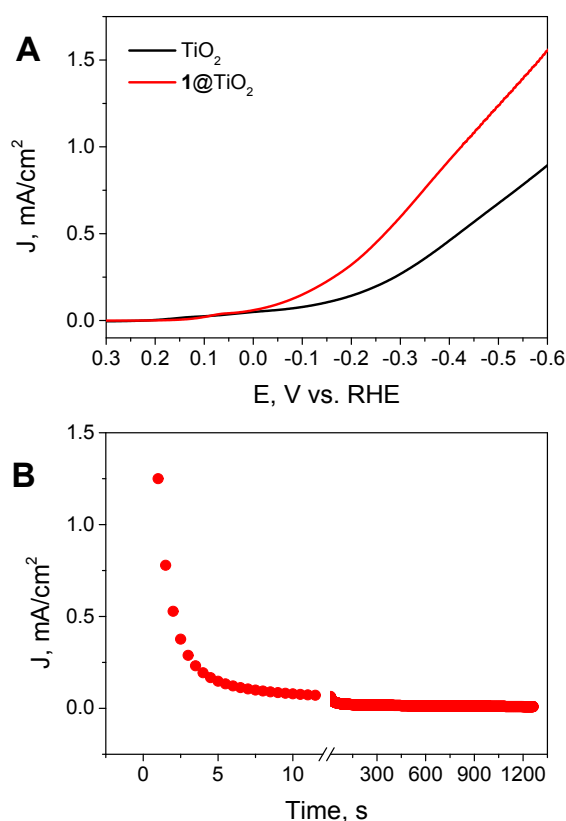


Figure 6. (A) J-V curves of bare TiO<sub>2</sub> and **1@TiO<sub>2</sub>** in 0.1 M Na<sub>2</sub>SO<sub>4</sub> (pH 3), scan rate  $v = 100 \text{ mV/s}$ ; (B) chronoamperometry of **1@TiO<sub>2</sub>** in 0.1 M Na<sub>2</sub>SO<sub>4</sub> (pH 3) at  $-0.5 \text{ V}$  vs RHE.

In order to test the catalytic ability of **1@TiO<sub>2</sub>** under operative conditions, chronoamperometry experiments have been conducted (Figure 6B). After application of a constant potential of  $-0.94 \text{ V}$  vs. SCE at pH 3 ( $-0.5 \text{ V}$  vs. RHE) a rapid abatement of the catalytic current is observed within the first minute electrolysis until a current density of  $\sim 10 \mu\text{A/cm}^2$  is reached after ca 30 minutes.

The rapid loss of catalytic activity can be mostly related to leaching of nickel complex from the TiO<sub>2</sub> surface. As a matter of fact, treatment of the electrodes with 0.1 M NaOH after 30 minutes electrolysis shows that only traces of nickel complex **1** (<1% of the initial amount) are still present on the TiO<sub>2</sub> surface. Whether catalyst loss is due to simple dissolution triggered by the negative applied bias§§ or is related to inactivation under catalytic conditions an open question. Regardless of the actual reason, direct application of **1** in a heterogeneous system does not lead to valuable results as observed in the homogeneous phase. Similar conclusions were recently drawn for a related complex covalently attached to a glassy carbon electrode.<sup>35</sup> It is worth noting, however, that the behaviour of **1** onto a metal oxide electrode is apparently different from that observed for a nickel bis(diphosphine) analogue based on phosphonic acid anchoring groups.<sup>31a</sup> To this respect, the different binding mode (phosphonic vs. carboxylic acid groups) very likely favours a more stable binding and thus improved activity towards hydrogen evolution in aqueous solution. Nevertheless, a substantial current abatement was observed also in the that case during continuous electrolysis within 1-2 hours.<sup>31a</sup> Furthermore, when other types of covalent attachment were considered,<sup>34,36</sup> in one case no (photo)electrochemical characterization was performed,<sup>34</sup> while in the other case the studies, limited to acetonitrile as the solvent, did not look in detail at long-term performances.<sup>36</sup> These observations thus suggest that the direct application of nickel bis(diphosphine) complexes in heterogeneous conditions is not as straightforward as in the homogeneous phase. As a matter of fact, other aspects that must be considered when molecular species are attached onto solid surfaces are the additional rigidity imparted to the catalyst as well as the proximity of the catalyst molecules. These features, induced by the surface grafting, might considerably alter the catalytic properties, particularly in the case of nickel bis(diphosphine) complexes, in which substantial conformational freedom is required for the pendant amine groups to positively assist the protonation steps needed for enhanced hydrogen evolution catalysis.<sup>24</sup> A careful evaluation of the functionalization strategy<sup>33</sup> is thus relevant in order to prepare suitable (photo)electrodes based on nickel bis(diphosphine) catalysts.

## Conclusions

A nickel(II) bis(diphosphine) complex bearing carboxylic acid groups (**1**) has been synthesized and characterized. Its catalytic ability towards hydrogen evolution has been tested under three different experimental conditions, namely in homogeneous electrocatalysis in acetonitrile with TFA as the proton source, in homogeneous photocatalysis in aqueous solutions using Ru(bpy)<sub>3</sub><sup>2+</sup> and ascorbic acid as the sensitizer and electron donor, respectively, and under heterogeneous electrochemical conditions upon direct grafting of **1** onto mesoporous TiO<sub>2</sub>. The results show that complex **1** behaves as an effective catalyst under homogeneous conditions, both electro- and photochemical ones. On the other hand, although a high surface coverage of TiO<sub>2</sub> films by complex **1** is attained, even

superior to previously reported strategies, **1** on TiO<sub>2</sub> is subjected to a rapid abatement of the HER catalysis. These results thus confirm how catalyst design must be tailored with respect to the conditions adopted, particularly when heterogeneous systems are considered. Accordingly, new strategies will be pursued in order to improve the stability and flexibility of nickel(II) bis(diphosphine) complexes on electroactive surfaces for application in energy conversion schemes.

## Conflicts of interest

There are no conflicts to declare.

## Acknowledgements

Financial support from the University of Ferrara (FAR2018, FAR2019) is gratefully acknowledged.

## Notes and references

‡ It should be considered that these efficiencies represent higher limiting values. Indeed, due to the partial superposition of the absorption of **1**, selective excitation of the ruthenium chromophore cannot be performed.

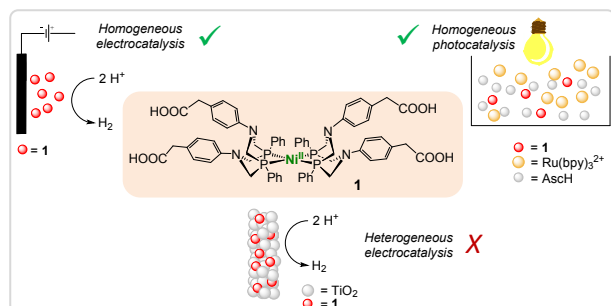
§ It should be remarked that, rather than ascorbic acid, the actual quencher is the ascorbate anion<sup>46,47</sup> which is almost exclusively present in aqueous solution at pH 5 (pK<sub>a</sub> = 4.1).

§§ No appreciable leaching of **1** is observed in the pH range 2-4 under open-circuit potential conditions.

- (a) V. Balzani, A. Credi and M. Venturi, *ChemSusChem*, 2008, **1**, 26. (b) N. Armaroli and V. Balzani, *Chem. Eur. J.*, 2016, **22**, 32.
- (a) N. S. Lewis and D. G. Nocera, *Proc. Natl. Acad. Sci. U.S.A.*, 2006, **103**, 15729. (b) D. G. Nocera, *Acc. Chem. Res.*, 2017, **50**, 616.
- J. C. Fontecilla-Camps, A. Volbeda, C. Cavazza and Y. Nicolet, *Chem. Rev.*, 2007, **107**, 4273.
- S. T. Stripp and T. Happe, *Dalton Trans.*, 2009, 9960.
- W. T. Eckenhoff, *Coord. Chem. Rev.*, 2018, **373**, 295.
- K. E. Dalle, J. Warnan, J. J. Leung, B. Reuillard, I. S. Karmel and E. Reisner, *Chem. Rev.*, 2019, **119**, 2752.
- V. Artero, G. Berggren, M. Atta, G. Caserta, S. Roy, L. Pecqueur and M. Fontecave, *Acc. Chem. Rev.*, 2015, **48**, 2380.
- C. Tard and C. J. Pickett, *Chem. Rev.*, 2009, **109**, 2245.
- (a) W. T. Eckenhoff, W. R. McNamara, P. Du and R. Eisenberg, *Biochim. Biophys. Acta*, 2013, **1827**, 958. (b) T. Lazarides, T. McCormick, P. Du, G. Luo, B. Lindley and R. Eisenberg, *J. Am. Chem. Soc.*, 2009, **131**, 9192. (c) T. M. McCormick, B. D. Calitree, A. Orchard, N. D. Kraut, F. V. Bright, M. R. Detty and R. Eisenberg, *J. Am. Chem. Soc.*, 2010, **132**, 15480.
- (a) N. Coutard, N. Kaeffer and V. Artero, *Chem. Commun.*, 2016, **52**, 13728. (b) N. Kaeffer, M. Chavarot-Kerlidou and V. Artero, *Acc. Chem. Res.*, 2015, **48**, 1286. (c) C. Baffert, V. Artero and M. Fontecave, *Inorg. Chem.*, 2007, **46**, 1817.
- (a) M. Natali, R. Argazzi, C. Chiorboli, E. Iengo and F. Scandola, *Chem. Eur. J.*, 2013, **19**, 9261. (b) E. Deponti and M. Natali, *Dalton Trans.*, 2016, **45**, 9136.
- C. H. Lee, D. K. Dogutan and D. G. Nocera, *J. Am. Chem. Soc.*, 2011, **133**, 8775.
- (a) R. M. Kellett and T. G. Spiro, *Inorg. Chem.*, 1985, **24**, 2373. (b) R. M. Kellett and T. G. Spiro, *Inorg. Chem.*, 1985, **24**, 2378.

- 14 M. Natali, A. Luisa, E. Iengo and F. Scandola, *Chem. Commun.*, 2014, **50**, 1842.
- 15 I. Bughun, I. Lexa and J. M. Savéant, *J. Am. Chem. Soc.*, 1996, **118**, 3982.
- 16 D. Khusnutdinova, A. M. Beiler, B. L. Wadsworth, S. I. Jacob and G. F. Moore, *Chem. Sci.*, 2017, **8**, 253.
- 17 N. Queyriaux, R. T. Jane, J. Massin, V. Artero and M. Chavarot-Kerlidou, *Coord. Chem. Rev.*, 2015, **304**, 3.
- 18 (a) Y. Sun, J. P. Bigi, N. A. Piro, M. L. Tang, J. R. Long and C. J. Chang, *J. Am. Chem. Soc.*, 2011, **133**, 9212. (b) M. Nippe, R. S. Khnazyer, J. A. Panetier, D. Z. Zee, B. S. Olaiya, M. Head-Gordon, C. J. Chang, F. N. Castellano and J. R. Long, *Chem. Sci.*, 2013, **4**, 3934. (c) R. S. Khnazyer, V. S. Thoi, M. Nippe, A. E. King, J. W. Jurs, K. A. El Roz, J. R. Long, C. J. Chang and F. N. Castellano, *Energy Environ. Sci.*, 2014, **7**, 1477.
- 19 S. Schnidrig, C. Bachmann, P. Muller, N. Weder, B. Spingler, E. Joliat-Wick, M. Mosberger, J. Windisch, R. Alberto and B. Probst, *ChemSusChem*, 2017, **10**, 4570.
- 20 F. Lucarini, M. Pastore, S. Vasylevskiy, M. Varisco, E. Solari, A. Crochet, K. M. Fromm, F. Zobi and A. Ruggi, *Chem. Eur. J.*, 2017, **23**, 6768.
- 21 (a) E. Deponti, A. Luisa, M. Natali, E. Iengo and F. Scandola, *Dalton Trans.*, 2014, **43**, 16345. (b) M. Natali, E. Badetti, E. Deponti, M. Gamberoni, F. A. Scaramuzzo, A. Sartorel and C. Zonta, *Dalton Trans.*, 2016, **45**, 14764. (c) N. A. Carmo dos Santos, M. Natali, E. Badetti, K. Wurst, G. Licini and C. Zonta, *Dalton Trans.*, 2017, **46**, 16455.
- 22 (a) C. L. Hartley, R. J. DiRisio, M. E. Screen, K. J. Mayer and W. R. McNamara, *Inorg. Chem.*, 2016, **55**, 8865. (b) N. A. Race, W. Zhang, M. E. Screen, B. A. Barden and W. R. McNamara, *Chem. Commun.*, 2018, **54**, 3290.
- 23 M. Tagliapietra, A. Squarcina, N. Hickey, R. De Zorzi, S. Geremia, A. Sartorel and M. Bonchio, *ChemSusChem*, 2017, **10**, 4430.
- 24 (a) A. D. Wilson, R. K. Shoemaker, A. Miedaner, J. T. Muckerman, D. L. DuBois and M. R. DuBois, *Proc. Natl. Acad. Sci. U.S.A.*, 2007, **104**, 6951. (b) M. O'Hagan, M.-H. Ho, J. Y. Yang, A. M. Appel, M. R. DuBois, S. Raugei, W. J. Shaw, D. L. DuBois and R. M. Bullock, *J. Am. Chem. Soc.*, 2012, **134**, 19409.
- 25 S. Wiese, U. J. Kilgore, D. L. DuBois and R. M. Bullock, *ACS Catal.*, 2012, **2**, 720.
- 26 U. J. Kilgore, J. A. S. Roberts, D. H. Pool, A. M. Appel, M. P. Stewart, M. R. DuBois, W. J. Dougherty, W. S. Kassel, R. M. Bullock and D. L. DuBois, *J. Am. Chem. Soc.*, 2011, **133**, 5861.
- 27 S. Wiese, U. J. Kilgore, M.-H. Ho, S. Raugei, R. M. Bullock, D. L. DuBois and M. L. Helm, *ACS Catal.*, 2012, **3**, 2527.
- 28 A. Dutta, D. L. DuBois, J. A. S. Roberts and W. J. Shaw, *Proc. Natl. Acad. Sci. U.S.A.*, 2014, **111**, 16286.
- 29 M. L. Helm, M. P. Stewart, R. M. Bullock, M. R. DuBois and D. L. DuBois, *Science*, 2011, **333**, 863.
- 30 (a) M. A. Gross, A. Reynal, J. R. Durrant and E. Reisner, *J. Am. Chem. Soc.*, 2014, **136**, 356. (b) B. C. M. Martindale, G. A. M. Hutton, C. A. Caputo and E. Reisner, *J. Am. Chem. Soc.*, 2015, **137**, 6018. (c) H. Kasap, C. A. Caputo, B. C. M. Martindale, R. Godin, V. W. Lau, B. V. Lotsch, J. R. Durrant and E. Reisner, *J. Am. Chem. Soc.*, 2016, **138**, 9183.
- 31 (a) T. E. Rosser, M. A. Gross, Y.-H. Lai and E. Reisner, *Chem. Sci.*, 2016, **7**, 4024. (b) M. A. Gross, C. E. Creissen, K. L. Orchard and E. Reisner, *Chem. Sci.*, 2016, **7**, 5537.
- 32 (a) B. Shan, B. D. Sherman, C. M. Klug, A. Nayak, S. L. Marquard, Q. Liu, R. M. Bullock and T. J. Meyer, *J. Phys. Chem. Lett.*, 2017, **8**, 4374. (b) D. Wang, M. V. Sheridan, B. Shan, B. H. Farnum, S. L. Marquard, B. D. Sherman, M. S. Eberhart, A. Nayak, C. J. Dares, A. K. Das, R. M. Bullock and T. J. Meyer, *J. Am. Chem. Soc.*, 2017, **139**, 14518.
- 33 (a) A. LeGoff, V. Artero, B. Joussemme, P. D. Tran, N. Guillet, R. Métayé, A. Fihri, S. Palacin and M. Fontecave, *Science*, 2009, **326**, 1384. (b) T. N. Huan, R. T. Jane, A. Benayad, L. Guetaz, P. D. Tran and V. Artero, *Energy Environ. Sci.*, 2016, **9**, 940.
- 34 G. F. Moore and I. Sharp, *J. Phys. Chem. Lett.*, 2013, **4**, 568.
- 35 A. K. Das, M. H. Engelhard, R. M. Bullock and J. A. S. Roberts, *Inorg. Chem.*, 2014, **53**, 6875.
- 36 (a) J. Seo, R. T. Pekarek and M. J. Rose, *Chem. Commun.*, 2015, **51**, 13264. (b) H. J. Kim, J. Seo and M. J. Rose, *ACS Appl. Mater. Interfaces*, 2016, **8**, 1061.
- 37 A. S. Weingarten, R. V. Kazantsev, L. C. Palmer, M. McClendon, A. R. Koltonow, A. P. S. Samuel, D. J. Kiebal, M. R. Wasielewski and S. I. Stupp, *Nat. Chem.*, 2014, **6**, 964.
- 38 B. J. Hathaway, D. G. Holah and A. E. Underhill, *J. Chem. Soc.*, 1962, 2444.
- 39 B. D. McCarthy, D. J. Martin, E. S. Rountree, A. C. Ullman and J. L. Dempsey, *Inorg. Chem.*, 2014, **53**, 8350.
- 40 V. Fourmond, P.-A. Jacques, M. Fontecave and V. Artero, *Inorg. Chem.*, 2010, **49**, 10338.
- 41 C. Costentin and J. M. Saveant, *ChemElectroChem*, 2014, **1**, 1226.
- 42 C. Costentin, S. Drouet, M. Robert and J. M. Saveant, *J. Am. Chem. Soc.*, 2012, **134**, 11235.
- 43 E. S. Rountree and J. L. Dempsey, *J. Am. Chem. Soc.*, 2015, **137**, 13371.
- 44 V. Artero and J.-M. Saveant, *Energy Environ. Sci.*, 2014, **7**, 3808.
- 45 M. Razavet, V. Artero and M. Fontecave, *Inorg. Chem.*, 2005, **44**, 4786.
- 46 A. Reynal, E. Pastor, M. A. Gross, S. Selim, E. Reisner and J. R. Durrant, *Chem. Sci.*, 2015, **6**, 4855.
- 47 M. Natali, *ACS Catal.*, 2017, **7**, 1330.
- 48 L. A. Kelly and M. A. J. Rodgers, *J. Phys. Chem.*, 1994, **98**, 6377.
- 49 <https://sdbcs.db.aist.go.jp>. National Institute of Advanced Industrial Science and Technology, 2018.

## Table of content entry



A nickel(II) bis(diphosphine) complex bearing carboxylic acid groups has been tested as a catalyst for hydrogen evolution under different conditions.